

12th National Conference  
on Earthquake Engineering  
Salt Lake City, Utah  
27 June - 1 July 2022

Hosted by the Earthquake Engineering Research Institute

## Seismic Risk to Buildings in the San Francisco Bay Area Predicted by Broadband Physics-based M7.0 Hayward Fault Rupture Simulations

M. Kenawy<sup>1</sup>, D. McCallen<sup>2,3</sup>, A. Pitarka<sup>4</sup>, and A. Rodgers<sup>5</sup>

### ABSTRACT

Physics-based earthquake fault rupture simulations offer new opportunities to study the impacts of large and rare earthquake events on the built environment. Structures located near active faults experience shaking that is sensitive to earthquake source characteristics, wave propagation patterns and site conditions. Three-dimensional deterministic simulations inherently incorporate such characteristics, but the associated computational expenses typically impose limitations on the model parameters. In this study, we use three-dimensional earthquake simulations and nonlinear structural models to examine the demands imposed on building structures across a regional domain representing the San Francisco Bay Area due to a M7.0 Hayward Fault rupture, and the impacts of radiation patterns and modeled wavespeeds on these demands. We show that the response of building structures is sensitive to the underlying soil representation, especially west of the Hayward Fault. Because of the interaction of the fault rupture directivity with the complex shear wave velocity profile near the fault, structures may be subjected to high intensity shaking and significant damage both east and west of the fault.

### Introduction

Urban areas near active earthquake faults are at a high risk of experiencing disruptive and costly earthquake events. The Hayward fault is considered one of the most dangerous earthquake faults in the United States because it runs through the highly urbanized and densely populated San Francisco Bay Area (SFBA). Recent studies have predicted that the Hayward fault is likely to rupture in a magnitude 6.8 - 7.0 scenario in the next 30 years and significantly impact the SFBA infrastructure and economy, with estimated losses of about \$82 billion dollars [1]. Understanding the risks imposed by such a scenario can help guide community planning, structural retrofits, and other preparedness measures to reduce the impacts of a future Hayward fault earthquake.

Preparing for large earthquake events poses significant challenges on the engineering community because few recordings are available for such events, making them difficult to predict using statistical ground motion models [2]. In addition, ground shaking near rupturing faults is particularly sensitive to the rupture characteristics, the seismic wave propagation patterns, and soil conditions [3]. In light of these challenges, deterministic earthquake simulations have emerged as an alternative to the use of empirical ground motion models, enabling seismologists to represent the physics of fault rupture (source effects), three-dimensional wave propagation patterns (path effects), and the interaction between the seismic waves and near-surface soil deposits (site effects). Physics-based fault rupture simulation methods have been evolving rapidly in recent years, and were used in several studies to analyze the response of structures to

---

<sup>1</sup> Postdoctoral Scholar, University of Nevada, Reno, 1664 N Virginia St, Reno, NV 89557 (mmkenawy@ucdavis.edu)

<sup>2</sup> Professor, University of Nevada, Reno, 1664 N Virginia St, Reno, NV 89557

<sup>3</sup> Senior Scientist, Lawrence Berkeley National Laboratory, 1 Cyclotron Rd, Berkeley, CA 94720

<sup>4</sup> Seismology Deputy Group Leader, Lawrence Livermore National Laboratory, 7000 East Ave, Livermore, CA 94550

<sup>5</sup> Staff Scientist, Lawrence Livermore National Laboratory, 7000 East Ave, Livermore, CA 94550

earthquakes [3-7]. However, fully deterministic, broadband, three-dimensional ground motion simulations representing a wide range of frequencies, require a substantial computational effort to cover large regional domains with the discretization granularity required to simulate frequencies of engineering interest. Such simulations are becoming more feasible using high-performance computing tools, yet some limitations persist on the maximum frequency and soil conditions that can feasibly be represented in the simulation, especially if a large number of simulations is needed. For example, it is computationally expensive to represent near-surface material properties with low shear wavespeeds for large domains, while obtaining the desired high frequency. Consequently, it is common to utilize artificially high minimum shear wavespeeds in fault rupture simulations. The impact of this idealization on the predicted ground motion intensity and corresponding risk to infrastructure is not fully understood. A detailed understanding of the impacts of the idealizations in earthquake simulations is important not only for appropriate interpretation of future earthquake risks, but also for prioritization of the available computational resources.

In this study, we use M7.0 Hayward fault rupture simulations to examine the seismic risk to low, mid and high-rise building structures across the SFBA, and explore two important engineering questions: (1) what are the impacts of the complex path and site characteristics in the earthquake simulations on the risks to building structures near the fault? And (2) how does the assumed minimum shear wavespeed in the simulation affect the predicted demands on structures? We use our preliminary findings to make recommendations for the future development of deterministic fault rupture simulations for engineering risk assessments.

### M7.0 Hayward fault simulations

The simulations were conducted as part of the EQSIM (Earthquake Simulation Framework for Physics-Based Fault-to-Structure Simulations) application development under the U.S. Department of Energy Exascale Computing Project [8]. Broadband ground motions were generated based on a fully deterministic wave propagation modeling approach using the finite difference code SW4 [9] which simulates seismic waves using 3D earth models on distributed-memory parallel computers. The kinematic earthquake rupture modeling technique of Graves and Pitarka was used to simulate the fault rupture processes [10, 11, 12]. Two different M7.0 strike-slip rupture realizations of the Hayward fault were simulated on the Summit Supercomputer at Oak Ridge National Laboratory (ORNL) over a regional domain of 120 x 80 x 30 km representing the SFBA geological features, based on the 3D model developed by the U.S. Geological Survey (USGS). Further description of the simulation technique is available in Rodgers et al. [13]. The two realizations are identical apart from two primary differences in the highest resolved frequency and lowest represented wavespeeds: in scenario A, frequencies up to 10Hz are resolved and the minimum shear wavespeed is 500 m/s, whereas scenario B resolves frequencies up to 5Hz and a minimum shear wavespeed of 250 m/s. The ground motion fault-normal (FN) components and fault-parallel (FP) components are sampled at 2,301 surface stations. The median, 5<sup>th</sup> percentile and 95<sup>th</sup> percentile pseudo acceleration spectra (SA) associated with the FN component are shown in Fig. 1a. Due to the imposed minimum shear wavespeed, neither scenario fully honors the near-surface low wavespeed sediments consistent with the USGS representation of the Franciscan complex west of the fault. This area, which includes cities such as Oakland, Berkeley and Hayward, may have near-surface wavespeeds as low as 100 m/s. The surface geological properties of the SFBA are highlighted in Fig. 1b in a map representation of the average shear wave velocity in the upper 30 meters of soil ( $V_{s30}$ ), where the low velocity sediments on the San Francisco Bay margins are evident.

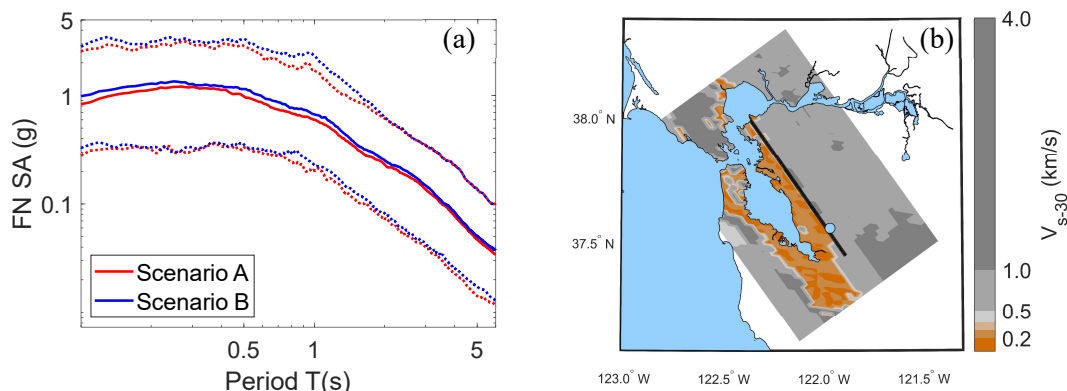


Figure 1. (a) Pseudo acceleration response spectra of the FN ground motion component of scenarios A and B within 10 km of the fault; (b) map of  $V_{s30}$  over the SFBA as represented in the USGS model.

### **Properties of the building simulation models**

Three reinforced concrete buildings were designed following the provisions of ASCE 7-16 [14] and ACI 318-14 [15]: a 3-story, a 12-story, and a 20-story building. The seismic design is based on the risk-targeted maps for a site that is approximately two kilometers away from the Hayward fault in Berkeley with site class C. Two-dimensional simulation models of representative building frames were created using OpenSees [16] using nonlinear hinge models that are capable of representing inelastic behavior. The first-mode periods of the 3-story, 12-story and 20-story buildings are 0.75 s, 2.23 s and 3.45 s, respectively. Dynamic analyses of the buildings over the full SFBA domain subjected to the FN and FP ground acceleration components of scenarios A and B were conducted in a set of parallel simulations using the CORI computer at Lawrence Berkeley National Laboratory (LBNL). Further details about the structural modeling parameters are available in Kenawy et al. [3].

### **Distribution of structural demands due to FN and FP ground motion components**

Previous studies on simulated ruptures of the Hayward fault have demonstrated that ground motion intensities tended to be higher on the east side than on the west side of the fault in selected frequency ranges. This asymmetry was attributed to several factors, including the deeper low wavespeeds in the sedimentary Great Valley Sequence east of the fault, compared to the shallower low wavespeed in the sediments overlaying the Franciscan Complex west of the fault, and the east-dipping nature of the fault resulting in hanging-wall effects [17]. Maps of ground motion intensity parameters and the corresponding structural demands in this study are consistent with those findings. Examples of the structural demands on the 3-story building, represented by maps of the maximum interstory drift ratio (MIDR), are shown in Fig. 2a and 2b. The map trends suggest the presence of complex interaction between the geological properties and the wave propagation patterns, impacting the structural demands around the Hayward fault. Comparison of the structural risk trends associated with the FN and FP components indicates that the structural demands associated with the FP ground motion component may be up to 40% higher than the FN component. This is in contrast to the results of previous studies [3] conducted on domains with relatively simplistic geology, in which the directivity effects associated with the FN component typically resulted in the highest structural demands. Furthermore, in the simulations conducted in this study, the highest structural demands associated with the FN component were confined to a 5 km distance from the fault, with some symmetry around the fault, and the higher demands concentrated toward the end of the rupture (north-west). On the other hand, the highest structural demands associated with the FP component are generally further away from the fault (within 15-20 km) and toward the middle of the rupture. These results point to systematic differences between the structural demand trends associated with the FN and FP components in the presence of complex geology that should be accounted for in the analysis of structures within a 20 km distance from the fault.

The differences between the FN and FP component trends are further illustrated in Fig. 2c, in which the ratio of the demands associated with the FP and FN components are plotted for the 3-story building. The demands associated with the FP component are 1.1 – 2 times higher than those associated with the FN component over most of the domain (orange to red), and in some localized regions far from the rupture directivity range near the fault, the ratio between the FP and FN demands is between 2 and 5 (dark red). The FN demands are higher than the FP demands mostly in narrow strips around the fault in the forward and backward directivity regions (green color). Similar maps for the 12-story and 20-story buildings reveal that the FP/FN MIDR ratio is higher for stiffer buildings, which implies higher sensitivity of the low-rise buildings to the site conditions and geological properties compared to the high-rise buildings.

### **Impact of minimum shear wavespeed**

Although Scenarios A and B differ in the maximum resolved frequency, the difference in the frequency range (5 to 10Hz) is only expected to impact very stiff structures, which are not considered in this study. Therefore, comparisons between the demands associated with both scenarios for our purposes primarily indicate the effects of using a lower minimum wavespeed in the simulation. These effects are illustrated in Fig. 3, which shows maps of the ratio of the MIDR associated with Scenario B over Scenario A. The maps show the amplification of structural demands west of the fault for all three building types when a lower minimum wavespeed is employed in the simulation, thus better representing the effects of the near-surface sediments overlaying the Franciscan Complex. The demands associated with a 250 m/s minimum speed in the Franciscan Complex are mostly between 1.1 and 2 times the demands associated with a 500 m/s minimum speed, but in some areas as high as 3 times. On the other hand, reducing the minimum wavespeed does not affect the structural demands on the east side of the fault because the surface wavespeeds are

generally high (refer to Fig.1b). Finally, the amplification due to reducing the minimum wavespeed is higher for the 3-story building than the 12-story and 20-story buildings. This is consistent with the SA trends observed for both scenarios in Fig. 1a, which indicate higher SA in scenario B within the period range between 0.2 and 2 s, but very similar SA for periods longer than 2 s. These results also suggest that stiffer buildings may be more sensitive to the representation of the velocity structure in earthquake simulations than flexible buildings.

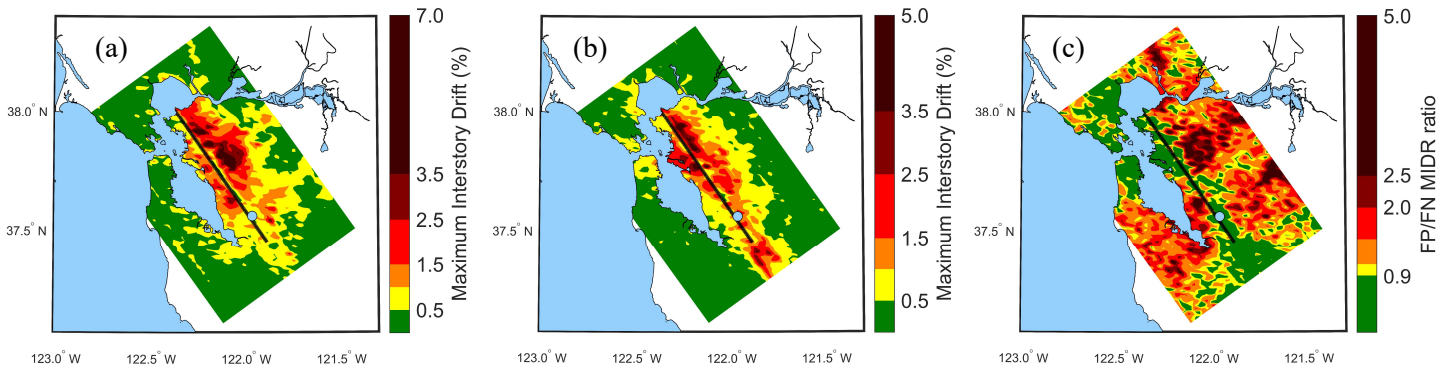


Figure 2. Map representation of the MIDR on the 3-story building associated with (a) the FP component, and (b) the FN component; (c) ratio of the FP to FN 3-story MIDR. The light blue circle represents the epicenter.

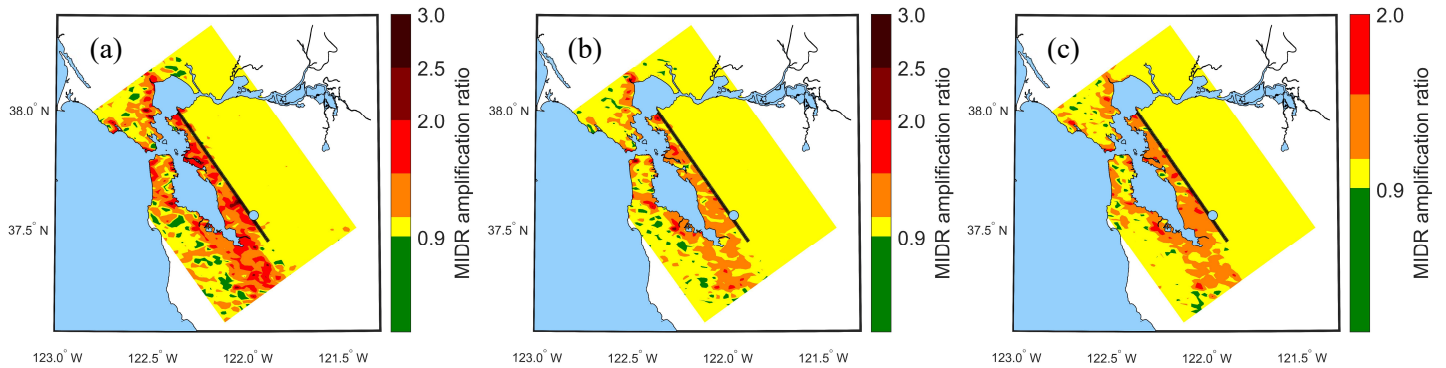


Figure 3. Maps representing the ratio of the MIDR of scenario B over scenario A across the SFBA for: (a) the 3-story building, (b) the 12-story building, and (c) the 20-story building.

### Conclusions

The seismic risk to building structures over the SFBA due to two M7.0 deterministic Hayward fault rupture simulations was examined, with focus on the path and site effects controlling the structural demands on buildings with different dynamic properties. Our preliminary findings show that the demands imposed by the FP component of ground motion can be significantly higher than the FN component, especially for areas east of and relatively far from the fault. Whereas the demands associated with the FN component appear to be controlled primarily by rupture directivity, the FP demands may be influenced more significantly by the complex geology near the Hayward fault. Finally, our analysis suggests that honoring the near-surface low shear wavespeed in the simulations is critical for predicting the risks to structures in urban areas west of the Hayward fault, especially for the analysis of stiffer structures. Therefore, we recommend that fault rupture simulations conducted for engineering risk assessments utilize minimum wavespeeds representative of those in the USGS model. Future simulations should also account for the nonlinear soil behavior that may dampen the ground motion intensity and reduce the predicted structural demands.

### Acknowledgments

This research was supported by the Exascale Computing Project, Project # 17-SC-20-SC, a collaborative effort of two U.S. Department of Energy organizations - the Office of Science and the National Nuclear Security Administration. Part of this work was performed at LBNL. Arben Pitarka's and Arthur Rodgers's work was performed by Lawrence Livermore National Laboratory under Contract DE-AC52-07NA27344. Support from the National Energy Research Scientific Computing Center at LBNL and the Oak Ridge Leadership Computing Facility at ORNL is acknowledged.

## References

1. Hudnut KW, Wein AM, Cox DA, Porter KA, Johnson LA, Perry SC, Bruce JL, LaPointe D. The HayWired earthquake scenario—We can outsmart disaster. US Geological Survey; 2018.
2. Campbell KW, Bozorgnia Y. NGA-West2 ground motion model for the average horizontal components of PGA, PGV, and 5% damped linear acceleration response spectra. *Earthquake Spectra*. 2014 Aug;30(3):1087-115.
3. Kenawy M, McCallen D, Pitarka A. Variability of near-fault seismic risk to reinforced concrete buildings based on high-resolution physics-based ground motion simulations. *Earthquake Engineering & Structural Dynamics*. 2021 May;50(6):1713-33.
4. Taborda R, Bielak J. Large-scale earthquake simulation: computational seismology and complex engineering systems. *Comput Sci Eng*. 2011;13(4):14-27.
5. Burks LS, Zimmerman RB, Baker JW. Evaluation of hybrid broadband ground motion simulations for response history analysis and design. *Earthq Spectra*. 2015;31(3):1691-1710.
6. Marafi NA, Eberhard MO, Berman JW, Wirth EA, Frankel AD. Impacts of simulated M9 Cascadia subduction zone motions on idealized systems. *Earthq Spectra*. 2019;35(3):1261-1287.
7. Bijelić N, Lin T, Deierlein GG. Evaluation of building collapse risk and drift demands by nonlinear structural analyses using conventional hazard analysis versus direct simulation with CyberShake seismograms. *Bull Seismol Soc Am*. 2019;109(5):1812-1828.
8. McCallen D, Petersson A, Rodgers A, Pitarka A, Miah M, Petrone F, Sjogreen B, Abrahamson N, Tang H. EQSIM—A multidisciplinary framework for fault-to-structure earthquake simulations on exascale computers part I: Computational models and workflow. *Earthquake Spectra*. 2021 May;37(2):707-35.
9. Sjögren B, Petersson NA. A fourth order accurate finite difference scheme for the elastic wave equation in second order formulation. *J Sci Comput*. 2012;52(1):17-48.
10. Graves R, Pitarka A. Kinematic ground-motion simulations on rough faults including effects of 3D stochastic velocity perturbations. *Bull Seismol Soc Am*. 2016;106(5):2136-2153.
11. Pitarka A, Graves R, Irikura K, Miyakoshi K, Rodgers A. Kinematic rupture modeling of ground motion from the M7 Kumamoto, Japan, earthquake. *Pure Appl Geophys*. 2019:1-23.
12. Graves R, Pitarka A. Validating ground-motion simulations on rough faults in complex 3-D media. In: *Proceedings of the 11th National Conference in Earthquake Engineering, EERI, Los Angeles, CA; 2018*.
13. Rodgers AJ, Pitarka A, McCallen DB. The effect of fault geometry and minimum shear wavespeed on 3D ground-motion simulations for an M w 6.5 Hayward fault scenario earthquake, San Francisco Bay Area, Northern California. *Bulletin of the Seismological Society of America*. 2019 Aug;109(4):1265-81.
14. *Minimum Design Loads and Associated Criteria for Buildings and Other Structures (ASCE/SEI 7-16)*. Reston, VA: American Society of Civil Engineers; 2017.
15. *Building Code Requirements for Structural Concrete (ACI 318-14)*. American Concrete Institute; 2014.
16. McKenna F, Fenves GL, Scott MH, et al. *Open System for Earthquake Engineering Simulation*. Berkeley, CA: University of California; 2000.
17. Rodgers AJ, Pitarka A, Petersson NA, Sjögren B, McCallen DB. Broadband (0–4 Hz) ground motions for a magnitude 7.0 Hayward fault earthquake with three-dimensional structure and topography. *Geophysical Research Letters*. 2018 Jan 28;45(2):739-47.